Microscopic structure of low-lying 0^+ states in the deformed ^{158}Gd

N. Lo Iudice,[1] A. V. Sushkov,[2] and N. Yu. Shirikova[2]
[1]*Dipartimento di Scienze Fisiche, Universitá di Napoli "Federico II" and Istituto Nazionale di Fisica Nucleare, Monte S Angelo, Via Cinthia I-80126 Napoli, Italy*
[2]*Bogoliubov Laboratory of Theoretical Physics, Joint Institute for Nuclear Research, 141980 Dubna, Russia*
(Received 30 September 2004; published 16 December 2004)

We study in the quasiparticle-phonon model the shell structure and the phonon content of the low-lying excited 0^+ states in ^{158}Gd. We show that the model accounts for the large abundance of 0^+ states observed in recent experiments and provides a detailed and exhaustive information about the properties of all these states, especially the extent and nature of their collectivity. This is achieved through an explicit investigation of the structure of the model wave functions and, more objectively, the calculation and comparative analysis of $E2$ and $E0$ transition probabilities, and, especially, two-nucleon transfer spectroscopic factors.

DOI: 10.1103/PhysRevC.70.064316 PACS number(s): 21.10.Jx, 21.10.Ky, 21.10.Re, 21.60.Jz

I. INTRODUCTION

The identification of a large number of low-lying 0^+ levels in the deformed ^{158}Gd, via a high resolution (p,t) experiment [1], has aroused a renewed interest toward 0^+ states. Similar (p,t) measurements, carried out with the same apparatus, have detected an equally large number of 0^+ levels in few deformed actinides [2] and in ^{168}Er [3], confirming the expectation that the abundance of low-lying 0^+ states is a common feature of several deformed nuclei.

The experiment has immediately stimulated theoretical studies. The first one was carried out within the interacting boson model (IBM) and the geometrical collective model (GCM) [4]. It was found that GCM and the traditional IBM approach, using monopole (s) and quadrupole (d) bosons, can yield only five 0^+ states below $\sim$3.2 MeV. If, however, dipole (p) and octupole (f) bosons are included in IBM, the model predicts about ten 0^+ states within the same energy range, close to the experimental number. It is reasonable to infer from the IBM analysis that a considerable number of detected states should be collective and few of them should have two-phonon octupole character.

A projected shell model (PSM) calculation has attempted to explain the nature of the observed states in terms of quasiparticle excitations [5]. In the PSM, one first generates a truncated spherical basis through projection from deformed Nilsson single-particle states and then uses such a basis to diagonalize a schematic interaction composed of monopole and quadrupole pairing plus a quadrupole-quadrupole interaction. The outcome of this calculation was that the 0^+ excitations are described by shell model states with either two-quasiparticle or four-quasiparticle dominant configurations. The same authors, however, point out that in order to increase the collectivity it should be necessary to mix the qp states with the vibrational motion.

We perform a microscopic calculation within the quasiparticle-phonon model (QPM) [6]. This generates microscopic phonons in random-phase approximation (RPA) and, then, diagonalizes a Hamiltonian composed of a sum of separable two-body potentials with different multipolarity in a basis of multiphonon states. Since both collective and non-collective RPA phonons are included in the multiphonon basis, the approach offers a less unbiased criterion for determining the nature of these 0^+ states. To this purpose we will try to provide a rather detailed characterization of them by computing energies, $E2$ and $E0$ transition strengths as well as spectroscopic factors.

The latter quantities have been extracted for all 0^+ states of ^{158}Gd just from the recently measured (p,t) cross sections [1] and are of the utmost interest. They are, in fact, unique probes of monopole [7] and quadrupole pairing vibrations [8]. Moreover, according to microscopic calculations carried out in BCS plus RPA [9], monopole and quadrupole pairing in combination with quadrupole particle-hole forces generate an asymmetry between (p,t) and (t,p) reactions. These studies, in fact, have predicted a low-lying oblate 0^+ pairing isomer strongly excited in (p,t) but not in (t,p) reactions, in accordance with experiments carried out on actinide nuclei [10].

A step beyond RPA has been made by the multiphonon calculations carried out within the QPM [11,12]. These were confined to the lowest lying 0^+ states. The present analysis will provide a more exhaustive information and will cover all 0^+ states.

II. BRIEF OUTLINE OF THE QPM

A. The Hamiltonian

The Hamiltonian has the following structure:

$$H = H_0 + V^{(P)} + V^{(M)}. \tag{1}$$

H_0 is the unperturbed one-body piece, $V^{(P)}$ and $V^{(M)}$ are the two-body potentials acting in the particle-particle (pp) and particle-hole (ph) channels.

The one-body Hamiltonian is composed of a kinetic term plus a one-body axially deformed Woods-Saxon potential $V_{\rm WS}(r,\beta_2,\beta_4)$, where β_2 and β_4 are the quadrupole and hexadecapole equilibrium deformation parameters. The single particle basis states generated by H_0 will be labeled by the asymptotic Nilsson quantum numbers $q=\{Nn_z\Lambda\uparrow\}$ for $K^\pi=\Lambda+1/2$ and $q=\{Nn_z\Lambda\downarrow\}$ for $K^\pi=\Lambda-1/2$.

The *ph* two-body interaction is composed of a sum of separable potentials of different multipolarity

$$V^{(M)} = -\sum_{\tau_1\tau_2}\sum_{\lambda\mu}\kappa_{\lambda\mu}^{(\tau_1\tau_2)}M_{\lambda\mu}^{\dagger}(\tau_1)M_{\lambda\mu}(\tau_2). \tag{2}$$

Here

$$M_{\lambda\mu} = R_{\lambda}(r)Y_{\lambda\mu}(\theta,\varphi) \tag{3}$$

is the λ-multipole field whose radial component $R_{\lambda}(r)$ is obtained as the derivative of the spherical WS potential. The coupling constants $\kappa_{\lambda\mu}^{(\tau_1\tau_2)}$ are related to the isoscalar ($T=0$) and isovector ($T=1$) strengths through

$$\kappa_{\lambda\mu}^{(pp)} = \kappa_{\lambda\mu}^{(nn)} = \frac{1}{2}(\kappa_{\lambda\mu}^{(T=0)} + \kappa_{\lambda\mu}^{(T=1)}),$$

$$\kappa_{\lambda\mu}^{(pn)} = \kappa_{\lambda\mu}^{(np)} = \frac{1}{2}(\kappa_{\lambda\mu}^{(T=0)} - \kappa_{\lambda\mu}^{(T=1)}). \tag{4}$$

The *ph* interaction includes, among other multipole terms, quadrupole-quadrupole as well as octupole-octupole potentials.

The *pp* interaction consists of a monopole plus a sum of multipole pairing potentials

$$V^{(P)} = -\sum_{\tau=p,n}G_0^{(\tau)}P_0^{\dagger}(\tau)P_0(\tau) - \frac{1}{2}\sum_{\lambda\neq 0\mu}\sum_{\tau=p,n}G_{\lambda}^{(\tau)}P_{\lambda\mu}^{\dagger}(\tau)P_{\lambda\mu}(\tau), \tag{5}$$

where

$$P_0^{\dagger} = \sum_q a_q^{\dagger}a_{\bar{q}}^{\dagger}, \tag{6}$$

$$P_{\lambda\mu}^{\dagger} = \sum_{q_1q_2} f_{\lambda\mu}(q_1q_2)a_{q_1}^{\dagger}a_{\bar{q}_2}^{\dagger} \tag{7}$$

are, respectively, the monopole and λ multipole pairing operators. In the above equations, $\bar{q}$ denotes time reversal conjugation and

$$f_{\lambda\mu}(q_1q_2) = \langle q_1|M_{\lambda\mu}|q_2\rangle. \tag{8}$$

B. QPM procedure

The QPM procedure goes through the following steps.

(a) Express the Hamiltonian in terms of quasiparticle creation ($\alpha_q^{\dagger}$) and annihilation (α_q) operators by means of the Bogoliubov canonical transformation

$$a_q = u_q\alpha_q + v_q\alpha_{\bar{q}}^{\dagger}. \tag{9}$$

(b) Construct the RPA phonon operators

$$Q_{i\nu}^{\dagger} = \frac{1}{2}\sum_{q_1q_2}(\psi_{q_1q_2}^{i\nu}\alpha_{q_1}^{\dagger}\alpha_{\bar{q}_2}^{\dagger} - \phi_{q_1q_2}^{i\nu}\alpha_{q_1}\alpha_{\bar{q}_2}), \tag{10}$$

whose amplitudes satisfy the normalization condition

$$\sum_{q_1q_2}[(\psi_{q_1q_2}^{i\nu})^2 - (\phi_{q_1q_2}^{i\nu})^2] = \frac{2}{1+\delta_{\nu 0}}. \tag{11}$$

For $\nu=K^{\pi}=0^+$, we have to separate the ghost states from the physical ones. In the presence of monopole and quadrupole pairing, imposing the vanishing of the lowest 0^+ RPA root yields the following equations for protons ($\tau=p$) and neutrons ($\tau=n$) [11]

$$\sum_q^{(\tau)}\frac{\Delta_q}{E_q\Delta_0} = \frac{2}{G_0}, \quad \sum_q^{(r)}\frac{f_{20}(qq)\Delta_0}{2E_q\Delta_2} + \sum_{q_1q_2}^{(r)}\frac{[f_{20}(q_1q_2)v_{q_1q_2}^{(+)}]^2}{E_{q_1}+E_{q_2}} = \frac{1}{G_{20}}, \tag{12}$$

where

$$E_q = \sqrt{(\epsilon_q-\lambda_{\tau})^2+\Delta_q^2}, \quad v^{(\pm)} = u_{q_1}u_{q_2} \pm v_{q_1}v_{q_2}, \tag{13}$$

$$\Delta_q = \Delta_0 + f_{20}(qq)\Delta_2. \tag{14}$$

The quantities

$$\Delta_0 = G_0\sum_q u_qv_q, \quad \Delta_2 = G_{20}\sum_q f_{20}(qq)u_qv_q \tag{15}$$

are the monopole and quadrupole pairing gaps, respectively. Equations (12), together with the number conserving condition

$$N^{(\tau)} = \sum_q^{(\tau)}\left[1-\frac{\epsilon_q-\lambda_{\tau}}{E_q}\right], \tag{16}$$

determine the Bogoliubov amplitudes u_q and v_q for the $K^{\pi}=0^+$ states.

(c) Express the starting Hamiltonian in terms of the RPA phonons by making use of the above definitions. The final outcome of this step is the interacting phonon Hamiltonian

$$H_{\mathrm{QPM}} = \sum_{v_i}\omega_{v_i}Q_{v_i}^{\dagger}Q_{v_i} + H_{vq}, \tag{17}$$

where $v_i=\{i\lambda_i\mu_i\}$. The first term is an unperturbed Boson Hamiltonian diagonal in the basis of the RPA phonon states $|v_i\rangle = Q_{v_i}^{\dagger}|0\rangle$ of energies ω_{v_i}. These are coupled by the term H_{vq}.

(d) Put the interacting phonon Hamiltonian in diagonal form through the variational principle using the trial wave function

$$\Psi_{\nu K^{\pi}=0^+} = \sum_i C_i(\nu)|i,K^{\pi}=0^+\rangle + \sum_{v_1v_2}C_{v_1v_2}(\nu)|[v_1\otimes v_2]_{0^+}\rangle, \tag{18}$$

where $|i,K^{\pi}=0^+\rangle = Q_{i20}^{\dagger}|0\rangle$ are the 0^+ phonons and

$$|[v_1\otimes v_2]_{0^+}\rangle = [Q_{v_1}^{\dagger}\otimes Q_{v_2}^{\dagger}]_{0^+}|0\rangle \tag{19}$$

the two-phonon basis states. This basis contains phonons of different multipolarity, including the octupole ones.

Each intrinsic $K^{\pi}=0^+$ state defines a band whose members, in the strong coupling limit, are described by the total wave function

$$\Psi^I_{nMK} = \sqrt{\frac{2I+1}{8\pi^2}} D^I_{M0} \Psi_{nK^\pi=0^+}, \tag{20}$$

where the D^I_{MK} are the Wigner wave functions. The observed $I^\pi=0^+$ levels are described by the $I=0$ bandhead states of the $K^\pi=0^+$ bands.

Using this wave function, we obtain for the reduced strength of the electric monopole and quadrupole transitions ($\lambda=0,2$)

$$\begin{aligned} B(E\lambda; I=0K^\pi_\nu=0^+_\nu \rightarrow I=\lambda K_0=0^+_0) &= \left| \langle 0^+_0 | \sum_k e_{\rm eff}(k) r^2_k Y_{\lambda 0} | 0^+_\nu \rangle \right|^2 \\ &= \left| \sum_i C^{(\nu)}_i \mathcal{M}^{(1)}_{0^+_i \rightarrow 0^+_0}(E\lambda) \right. \\ &\quad \left. + \sum_{\upsilon_1 \upsilon_2} C^{(\nu)}_{\upsilon_1 \upsilon_2} \mathcal{M}^{(2)}_{0^+_\nu \rightarrow 0^+_0}(E\lambda) \right|^2. \end{aligned} \tag{21}$$

Here $\mathcal{M}^{(1)}$ and $\mathcal{M}^{(2)}$ are the amplitudes of the transitions from one and two phonon components, respectively. They are given by

$$\begin{aligned} \mathcal{M}^{(1)}_{0^+_i \rightarrow 0^+_0}(E\lambda) = \sum_\tau e^{(i)}_{\rm eff}(\tau) \sum^\tau_{qq'} \langle q | r^2 Y_{\lambda 0} | q' \rangle (\psi^{(i)}_{qq'} + \varphi^{(i)}_{qq'}) \\ \times (u_q \upsilon_{q'} + \upsilon_q u_{q'}) \end{aligned} \tag{22}$$

and

$$\begin{aligned} \mathcal{M}^{(2)}_{0^+_\nu \rightarrow 0^+_0}(E\lambda) = \sum_\tau e^{(i)}_{\rm eff}(\tau) \sum^\tau_{qq'q_1} \langle q | r^2 Y_{\lambda 0} | q' \rangle (u_q u_{q'} - \upsilon_q \upsilon_{q'}) \\ \times (\psi^{(\upsilon_1)}_{q_1 q'} \varphi^{(\upsilon_2)}_{q_1 q} + \varphi^{(\upsilon_1)}_{q_1 q'} \psi^{(\upsilon_2)}_{q_1 q}). \end{aligned} \tag{23}$$

III. CALCULATION AND RESULTS

A. Numerical procedure

The first task in QPM is to generate the single particle basis states. This is done within the QPM scheme by choosing the parameters so as to reproduce the experimental energies and account for the electromagnetic properties of typical odd nuclei of the region under investigation [6,13]. For ^{158}Gd, the $A=155$ nuclei are usually chosen for this purpose. The above procedure fixes, in particular, the parameters of the deformed axially symmetric Woods-Saxon potential, including the deformation parameters β_2 and β_4, for a given set of the strength couplings of the different multipole potentials. The single particle spectrum was taken from the bottom of the well up to 5 MeV.

We constructed the phonon basis by including twenty $\lambda\mu=20$ phonons, yielding the corresponding RPA $K^\pi=0^+$ states, and ten phonons for each multipolarity $\lambda\mu=22$, 30, 31, 32, 33, 43, 44, 54, and 55. We used the $\lambda\mu=20$ piece of the quadrupole-quadrupole interaction, in addition to monopole plus quadrupole pairing, to generate the $K^\pi=0^+$ phonons. Both pairing terms were used to eliminate the $K^\pi=0^+$ ghost state through Eqs. (12). As discussed already, these equations determine the Bogoliubov u_q and υ_q amplitudes. For the other RPA phonons, we used only monopole pairing to compute these amplitudes, while the quadrupole pairing interaction was treated on the same footing as the *pp* potentials of multipolarity $\lambda \neq 2$. We used the *pp* and *ph* interactions of the appropriate multipolarity $\lambda\mu$ to generate the phonons of given $\lambda\mu$.

The strengths of the isoscalar *ph* separable interactions $\kappa^{(0)}_{\lambda\mu}$ were determined by a fit of the corresponding lowest experimental energy levels [14,15]. For the isovector strengths, we put $\kappa^{(1)}_{\lambda\mu} = -1.5\kappa^{(0)}_{\lambda\mu}$. An unambiguous criterion for fixing the multipole pairing strengths $G^{(\tau)}_{(\lambda\mu)}$, including the quadrupole pairing, is lacking. We put $G^{(\tau)}_{(\lambda\mu)} = G_{(\lambda\mu)} = \kappa^{(0)}_{\lambda\mu}$. For given values of the multipole pairing constants $G_{\lambda 0}$, the strength of the monopole pairing G_0 was fixed so as to reproduce the experimental odd-even mass differences. To compute the $E\lambda$ strengths, we used the effective charges $e^{(\lambda)}_{\rm eff}(p)=1.2$ and $e^{(\lambda)}_{\rm eff}(n)=0.2$

For ^{158}Gd, the deformation parameters deduced from the fit procedure are [13] $\beta_2=0.290$ and $\beta_4=0.06$. These lead to an overall good agreement with experiments for the lowest bands. In particular, for the γ band, one gets the energy $E_{2^+_\gamma}=1.2$ MeV and the $E2$ decay strength $B(E2; 2^+_\gamma \rightarrow 0^+_0) = 3.6$ (W.u.), in accordance with the corresponding experimental data $E^{(\rm exp)}_{2^+_\gamma}=1.187$ MeV and $B^{(\rm exp)}(E2; 2^+_\gamma \rightarrow 0^+_0) = 3.4$ (W.u.). As we shall see, the comparative analysis of the spectroscopic factors seems to favor the deformation parameters $\beta_2=0.257$ and $\beta_4=0.066$ determined in Ref. [16]. In correspondence of these latter parameters, we changed consistently a minimal set of two-body coupling constants, namely $\kappa_{20}(0)=G_{20}=0.0178$ and $\kappa_{22}(0)=0.0195$ in fm^2 MeV^{-1}. We obtained an equally good agreement with experiments for the lowest bands. In particular, for the γ band, we got $E_{2^+_\gamma}=1.18$ MeV and the $E2$ decay strength $B(E2; 2^+_\gamma \rightarrow 0^+_0)=3.9$ (W.u.), which compare equally well with the corresponding experimental data.

B. Spectra and e.m. transition strengths

As shown in Table I, RPA yields only 10 levels below 3.2 MeV. In order to obtain all the levels detected in the recent experiment [1], also shown in the table, we have to enlarge the phonon space by including at least the two-phonon states. Once we do so, we get about 14 levels below ~3.2 MeV, in accordance with experiments, and about 18 below ~3.5 MeV in agreement with the PSM results (Fig. 1). The QPM calculation overestimates the energies of the nearly degenerate levels located around 2 MeV, which are, instead, slightly underestimated by the PSM calculation [5].

The analysis of the phonon structure of the QPM states shows (Table I) that about six of them have a one-phonon character and one is a linear combination of one-phonon states. The others contain large, and in many cases dominant, two-phonon components. These are built out of collective octupole phonons in almost all cases, consistently with the IBM calculation [4]. Only two states contain large two-phonon components made out of $\lambda=4$ phonons, suggesting the need of including the *g* boson in the IBM scheme. The

TABLE I. Energies, $E2$ and normalized $E0$ strengths computed in QPM. The second and third columns give the experimental and RPA energies; the last column shows the weights C_i^2 of the phonon components in the QPM states. The symbol $[v]_i$ denotes either the one phonon $[\lambda\mu]_i$ or the two-phonon $[(\lambda\mu)_i\otimes(\lambda\mu)_j]_{0^+}$ components.

n	$E_n^{(\mathrm{exp})}$ (MeV)	$E_n^{(\mathrm{RPA})}$ (MeV)	E_n (MeV)	$B_n(E2)$ (W.u.)	ρ_n^2 ($\times 10^3$)	$[v]_i$	C_i^2
1	1.195	1.136	0.92	1.05	6.7	$[20]_1$	0.92
2	1.452	1.785	1.71	0.03	0.17	$[20]_2$	0.96
3	1.577	1.883	1.81	0.06	0.01	$[20]_3$	0.96
4	1.743	2.019	1.98	0.02	0.31	$[20]_4$	0.97
5	1.954	2.537	2.27	0.001	5.23	$[20]_5$	0.22
						$[20]_6$	0.28
						$[(31)_1\otimes(31)_1]_{0^+}$	0.37
6	1.96	2.630	2.39	0.007	2.99	$[20]_5$	0.15
						$[20]_6$	0.28
						$[(31)_1\otimes(31)_1]_{0^+}$	0.61
7	1.972	2.770	2.49	0.009	2.70	$[20]_5$	0.54
						$[20]_6$	0.38
8	2.277	2.893	2.68	0.015	0.29	$[20]_7$	0.88
9	2.338	2.980	2.72	0.001	0.00	$[(31)_1\otimes(31)_2]_{0^+}$	0.99
10	2.643	3.159	2.77	0.02	0.70	$[20]_8$	0.76
11	2.687	3.371	2.85	0.06	0.58	$[20]_9$	0.5
						$[(44)_1\otimes(44)_1]_{0^+}$	0.31
12	2.911		2.89	0.03	0.21	$[20]_9$	0.25
						$[(44)_1\otimes(44)_1]_{0^+}$	0.67
13	3.077		2.95	0.009	0.40	$[20]_{11}$	0.56
						$[(31)_1\otimes(31)_4]_{0^+}$	0.20
14	3.11		3.07	0.001	1.32	$[20]_{10}$	0.78
15			3.13	0.5×10^{-5}	0.00	$[(31)_2\otimes(31)_2]_{0^+}$	1.0

$E2$ decays of the 0^+ states to the 2^+ ground state are all weak (see also Fig. 2 lower panel). The largest strength is collected by the first excited 0_1^+ and is in good agreement with the experimental strength $B^{(\mathrm{exp})}(E2;0_1^+\rightarrow 2_0^+)=1.165$ W.u. [17]. The strength of the second 0_2^+, however, is orders of magnitude smaller than the measured one $B^{(\mathrm{exp})}(E2;0_2^+\rightarrow 2_0^+)=2.09$ W.u. The QPM strengths are smaller than the RPA values. This is expected because of the fragmentation induced by the phonon-phonon coupling. We find, however, against our expectations, that QPM and RPA $E2$ strengths are smaller than the ones obtained in the PSM [5]. The lack of quadrupole collectivity reflects the nature of our QPM and RPA 0^+ states, composed almost solely of pairing correlated $q\overline{q}$ components. The high energy ph configurations, responsible for enhancing the quadrupole correlations, play a very marginal role. The quenching with respect to the PSM quantities suggest some band mixing, accounted for in PSM but neglected in our scheme.

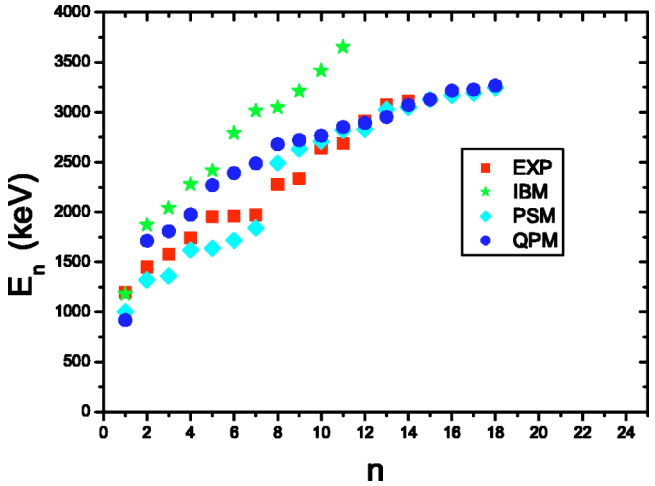

FIG. 1. (Color online) Energies of 0^+ states calculated in QPM for two different deformations compared to the experimental data and the levels calculated in PSM and IBM.

The lack of quadrupole collectivity in all RPA and QPM 0^+ states is further supported by the analysis of the normalized monopole transition strengths

$$\rho^2(E0;0_\nu^+\rightarrow 0_0^+)$$
$$=\frac{1}{e^2R_0^4}\left|\langle I=0K^\pi=0_0^+|\sum_k e_{\mathrm{eff}}(k)r_k^2|I=0K^\pi=0_\nu^+\rangle\right|^2$$
$$=\frac{4\pi}{e^2R_0^4}B(E0;I=0K_\nu^\pi=0_\nu^+\rightarrow I=0K_0=0_0^+). \quad (24)$$

All transitions resulted to be weak (Table I and upper panel

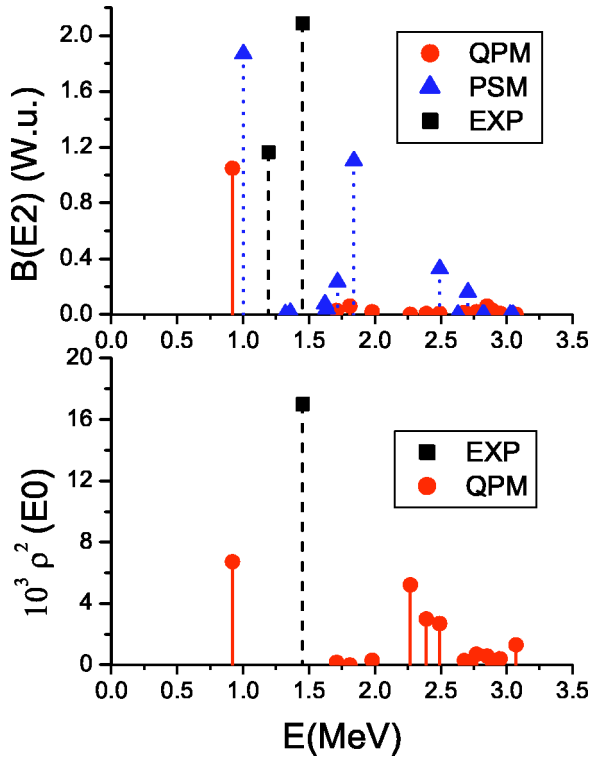

FIG. 2. (Color online) $E0$ and $E2$ strength distributions in ^{158}Gd.

of Fig. 2). All of them are much smaller than the typical β vibrational values $10^3\rho^2(E0;0^+_\beta\rightarrow 0^+_0)\sim 100$ [18,19]. The largest QPM $E0$ strength goes to the first 0^+_1, while the experimental one is mainly concentrated on the second 0^+_2 and is three times as large $[10^3\rho^2_{\rm exp}(E0;0^+_\beta\rightarrow 0^+_g)=17]$ [20].

For both $E0$ and $E2$ transitions, the distribution of the QPM strengths among the lowest two 0^+ levels is inverted with respect to experiments. In any case, the main conclusion to be drawn from the analysis of the two $E\lambda$ transitions remains valid. None of the detected 0^+ states is quadrupole collective. As already pointed out, these states are strongly pairing correlated. It is, indeed, expected on theoretical ground [19] that low-lying 0^+ states describe pairing vibrations [7–9]. Such an expectation is supported by the large or non-negligible spectroscopic factors obtained in the (p,t) transfer reaction experiments [1].

C. Two-nucleon transfer spectroscopic factors

To examine the (p,t) reaction data, we have computed the corresponding two-nucleon transfer spectroscopic amplitudes. These are defined as

$$\Gamma_\nu(p,t)=\langle 0^+_\nu,N-2|\sum_q^{(\tau=n)} a_q a_{\bar q}|0^+_0,N\rangle, \tag{25}$$

$$\Gamma_\nu(t,p)=\langle 0^+_\nu,N+2|\sum_q^{(\tau=n)} a^\dagger_q a^\dagger_{\bar q}|0^+_0,N\rangle, \tag{26}$$

for (p,t) and (t,p) reactions, respectively. For the ground to ground state transfer reactions we get

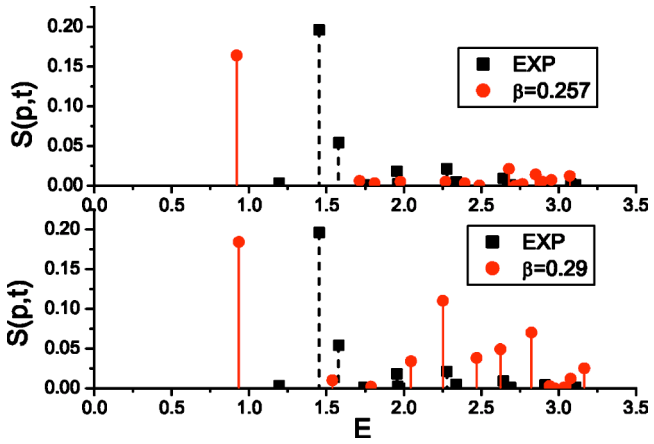

FIG. 3. (Color online) (p,t) spectroscopic factors computed in QPM for two different deformation parameters in ^{158}Gd.

$$\Gamma_0(p,t)=2\sum_q u_q(N-2)v_q(N)\simeq 2\sum_q u_q v_q, \tag{27}$$

$$\Gamma_0(t,p)=2\sum_q u_q(N+2)v_q(N)\simeq 2\sum_q u_q v_q=\Gamma_0(p,t), \tag{28}$$

where u_q and v_q stand for $u_q(N)$ and $v_q(N)$. For the transfer reactions to the excited states, the spectroscopic amplitudes take the form

$$\Gamma_\nu(p,t)=\sum_i C^{(\nu)}_i\Gamma_i(p,t),\quad \Gamma_\nu(t,p)=\sum_i C^{(\nu)}_i\Gamma_i(t,p), \tag{29}$$

where $\Gamma_i(p,t)$ and $\Gamma_i(t,p)$ are the RPA amplitudes

$$\Gamma_i(p,t)=\sum_{qq'}^{\tau=n}\Gamma_{[qq']_i}(p,t)\simeq 2\sum_{qq'}^{\tau=n}(-\psi^{(i)}_{qq'}v_q v_{q'}+\varphi^{(i)}_{qq'}u_q u_{q'}), \tag{30}$$

$$\Gamma_i(t,p)=\sum_{qq'}^{\tau=n}\Gamma_{[qq']_i}(t,p)\simeq 2\sum_{qq'}^{\tau=n}(\psi^{(i)}_{qq'}u_q u_{q'}-\varphi^{(i)}_{qq'}v_q v_{q'}). \tag{31}$$

The quantities to be compared with experiments are the spectroscopic factors normalized to the ground state transfer strengths

$$\mathcal{S}_\nu(p,t)=\left(\frac{\Gamma_\nu(p,t)}{\Gamma_0(p,t)}\right)^2,\quad \mathcal{S}_\nu(t,p)=\left(\frac{\Gamma_\nu(t,p)}{\Gamma_0(t,p)}\right)^2. \tag{32}$$

As shown in Fig. 3, the QPM spectrum is in overall agreement with the measured one. Indeed, the calculation yields a large strength for only one low-lying 0^+ state and small but non-negligible strengths for most of the other states, consistently with the experiments. Moreover, as shown in Table II, the QPM strengths add up to 24% of the ground state spectroscopic factor, very close to the experimental value ~25%.

TABLE II. Energies, (pt) and (tp) spectroscopic factors computed in QPM, compared with the available corresponding experimental quantities.

	Expt.		QPM			QPM ($\beta_2=0.29$)	
n	E_n (MeV)	$\mathcal{S}_n(p,t)$	E_n (MeV)	$\mathcal{S}_n(p,t)$	$\mathcal{S}_n(t,p)$	E_n (MeV)	$\mathcal{S}_n(p,t)$
1	1.195	0.003	0.919	0.164	0.529	0.933	0.184
2	1.452	0.196	1.711	0.006	0.03	1.538	0.010
3	1.577	0.003	1.809	0.003	0.01	1.786	0.002
4	1.743	0.001	1.976	0.005	0.0005	2.046	0.034
5	1.954	0.018	2.268	0.005	0.009	2.252	0.110
6	1.960	0.002	2.391	0.003	0.009	2.469	0.038
7	1.972	0.0	2.488	0.0	0.08	2.624	0.049
8	2.277	0.021	2.679	0.02	0.002	2.823	0.071
9	2.338	0.005	2.719	0.0	0.0007	2.939	0.003
10	2.643	0.009	2.766	0.002	0.07	2.972	0.0
11	2.688	0.001	2.851	0.014	0.007	3.036	0.001
12	2.911	0.004	2.891	0.005	0.005	3.077	0.012
13	3.077	0.002	2.953	0.007	0.004	3.166	0.025
14	3.110	0.001	3.072	0.012	0.005	3.248	0.002
$\Sigma_n S_n(p,t)$		$\sim$0.25		$\sim$0.24	$\sim$0.76		$\sim$0.54

Nonetheless, an important discrepancy concerning the lowest two 0^+ states emerges from a more detailed analysis of the figure (see also Table II). The QPM strength is large for the lowest 0_1^+ and negligible for the second 0_2^+, exactly the opposite of the experimental findings. This discrepancy is quite analogous to the one concerning the $E0$ and $E2$ transitions.

The phonon composition of the QPM states does not give any information on the way pairing correlations affect the two-nucleon transfer amplitudes. To shed light on this mechanism, we need to explore the quasiparticle structure of the dominant RPA components of the low-lying QPM 0^+ states. We found, first of all, that almost only paired $q\bar{q}$ configurations enter into the 0^+ states. Hence, the RPA spectroscopic amplitudes (30) are given by

$$\Gamma_i(p,t) \simeq -2\sum_q^{\tau=n} [\psi_q^i v_q^2 - \phi_q^i u_q^2], \tag{33}$$

$$\Gamma_i(t,p) \simeq 2\sum_q^{\tau=n} [\psi_q^i u_q^2 - \phi_q^i v_q^2]. \tag{34}$$

We show some typical cases in Table III. The first two 0^+ contains a very large number of two-quasiproton and two-quasineutron states. The largest forward amplitudes ψ of the first 0_1^+ have all the same (negative) sign. The second 0_2^+, instead, has a comparable number of positive and negative amplitudes. As a result, all main components contribute coherently to the spectroscopic amplitude in the first 0_1^+ and interfere destructively in the second 0_2^+. This is illustrated in Fig. 4. The figure shows also the quite significant contribution of the small amplitude (<0.08) components in the case of the 0_1^+. This contribution adds up coherently with the one due to the large amplitude components. The small amplitude components play a less important role in the other 0_2^+ state.

Table III shows two additional typical states. The 0_3^+ is a neutron excitation due to few two-quasineutron states whose amplitudes have opposite sign. Hence a small (p,t) transfer strength is obtained. The 0_4^+ RPA phonon is mainly a proton excitation, having only two neutron configurations of small amplitude. These, though having the same sign, are not sufficient to yield a sizable (p,t) strength.

Another important piece of information is provided by the plot in Fig. 5. The contribution of the "small" backward RPA amplitudes ϕ to $S(p,t)$ is comparable to, if not larger than, the one due to the "large" forward amplitudes. In the first 0_1^+, both amplitudes act coherently. In the second 0_2^+, instead, forward and backward amplitudes interfere destructively.

It is clear from this analysis that the mechanism through which pairing correlations affect the transfer transition strengths is a subtle and delicate one. Because of the presence of a large number of small amplitude configurations and important interference effects, the computed spectroscopic factors are highly sensitive to the parameters of the Hamiltonian. As shown in Table II, in going from $\beta_2=0.257$ to $\beta_2=0.290$, the magnitude and energy distribution of the QPM two-nucleon transfer spectroscopic factors change considerably as the energy increases. The ensuing QPM strengths are considerably larger than the experimental values. Hence the use of a slightly smaller β value. Such a choice does not affect the other properties of the low-lying intrinsic states.

For a more complete information, we have computed also the (t,p) spectroscopic factors. Table II shows that practically all the strength is concentrated in the first excited 0_1^+. No recent (t,p) data are available for ^{158}Gd. According to earlier experiments [21], the normalized spectroscopic factor

TABLE III. Two quasiparticle structure of selected $K^\pi=0^+$ RPA states. Only the large amplitude components are shown.

i	E_i (MeV)	$\Sigma^{(n)}_{q_1q_2}\psi^{(i)}_{q_1q_2}[(q_1)\otimes(q_2)]$	$\Sigma^{(p)}_{q_1q_2}\psi^{(i)}_{q_1q_2}[(q_1)\otimes(q_2)]$
1	1.136	$-0.468[(523\downarrow)\otimes(523\downarrow)]_n$	$-0.625[(411\uparrow)\otimes(411\uparrow)]_p$
		$-0.454[(521\uparrow)\otimes(521\uparrow)]_n$	$-0.224[(413\downarrow)\otimes(413\downarrow)]_p$
		$-0.245[(521\downarrow)\otimes(521\downarrow)]_n$	$+0.203[(532\uparrow)\otimes(532\uparrow)]_p$
		$-0.074[(642\uparrow)\otimes(642\uparrow)]_n$	$-0.197[(403\downarrow)\otimes(403\downarrow)]_p$
		$-0.206[(512\uparrow)\otimes(512\uparrow)]_n$	$+0.171[(541\uparrow)\otimes(541\uparrow)]_p$
		$-0.177[(633\uparrow)\otimes(633\uparrow)]_n$	$-0.190[(402\uparrow)\otimes(402\uparrow)]_p$
			$-0.151[(411\downarrow)\otimes(411\downarrow)]_p$
			$+0.145[(550\uparrow)\otimes(550\uparrow)]_p$
			$-0.122[(514\uparrow)\otimes(514\uparrow)]_p$
2	1.785	$0.340[(523\downarrow)\otimes(523\downarrow)]_n$	$-0.447[(411\uparrow)\otimes(411\uparrow)]_p$
		$-0.278[(651\uparrow)\otimes(651\uparrow)]_n$	$0.288[(413\downarrow)\otimes(413\downarrow)]_p$
		$-0.278[(642\uparrow)\otimes(642\uparrow)]_n$	$-0.197[(532\uparrow)\otimes(532\uparrow)]_p$
		$0.236[(521\uparrow)\otimes(521\uparrow)]_n$	$-0.189[(402\uparrow)\otimes(402\uparrow)]_p$
		$-0.217[(660\uparrow)\otimes(660\uparrow)]_n$	$0.179[(523\uparrow)\otimes(523\uparrow)]_p$
		$0.184[(505\uparrow)\otimes(505\uparrow)]_n$	$-0.153[(403\downarrow)\otimes(403\downarrow)]_p$
		$0.163[(512\uparrow)\otimes(512\uparrow)]_n$	
		$-0.122[(532\downarrow)\otimes(532\downarrow)]_n$	
3	1.883	$-0.742[(521\uparrow)\otimes(521\uparrow)]_n$	
		$+0.655[(523\downarrow)\otimes(523\downarrow)]_n$	
		$+0.104[(642\uparrow)\otimes(642\uparrow)]_n$	
4	2.019	$-0.146[(642\uparrow)\otimes(642\uparrow)]_n$	$-0.771[(413\downarrow)\otimes(413\downarrow)]_p$
		$-0.115[(651\uparrow)\otimes(651\uparrow)]_n$	$+0.358[(411\uparrow)\otimes(411\uparrow)]_p$
			$-0.234[(402\uparrow)\otimes(402\uparrow)]_p$
			$+0.187[(532\uparrow)\otimes(532\uparrow)]_p$
			$+0.138[(523\uparrow)\otimes(523\uparrow)]_p$
			$+0.127[(541\downarrow)\otimes(541\downarrow)]_p$
			$-0.125[(505\uparrow)\otimes(505\uparrow)]_p$

extracted from the measured (t,p) cross sections add up to $\Sigma\mathcal{S}_n(t,p)\sim 0.4$, about half the QPM total strength. On the ground of this result, we should therefore conclude that the 0^+ states of ^{158}Gd differ from the pairing isomeric states, which are populated only through (p,t) reactions, according to the predictions of Ref. [9] confirmed experimentally for the actinide nuclei [10]. On the other hand, for the suppression of the (t,p) transfer reaction it is required that (i) the contribution to the cross section comes mainly from oblate deformed Nilsson configurations and (ii) the RPA backward amplitudes can be neglected. According to the QPM calculation, none of these conditions is fulfilled in ^{158}Gd. Indeed, in our case, (i) a very large number of configurations with small amplitudes contribute to the cross section and (ii) the RPA backward amplitudes give a contribution comparable to the one due to the forward amplitudes.

IV. CONCLUDING REMARKS

We have performed a thorough investigation of the properties of the 0^+ states in ^{158}Gd by computing spectra, $E2$ as well as normalized $E0$ transition strengths, and, last but not

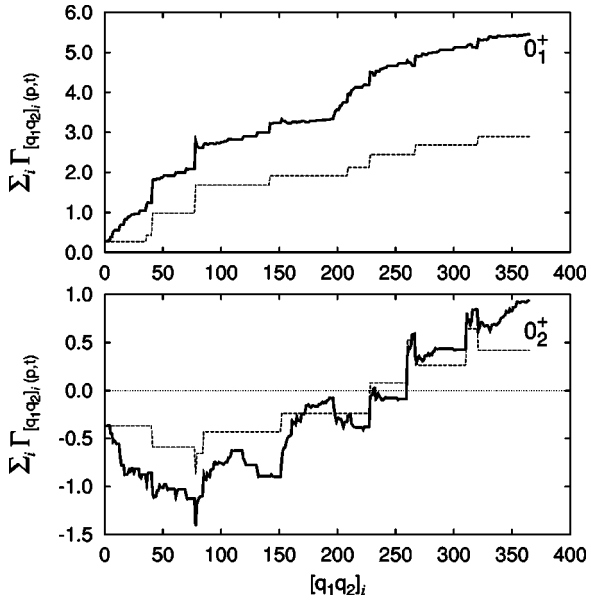

FIG. 4. Running sum of the two-quasiparticle amplitudes contributing to the RPA (p,t) spectroscopic factors in ^{158}Gd. The dashed line accounts for the contributions $|\Gamma_q|>0.08$ only.

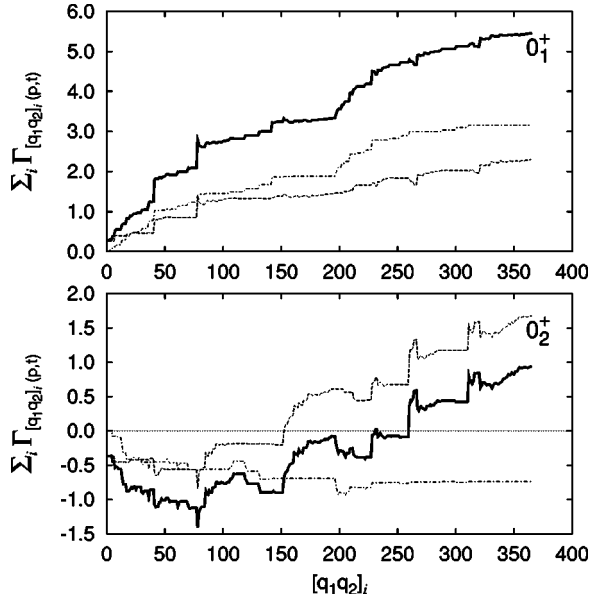

FIG. 5. The contribution to the running sum of the (p,t) transfer amplitudes coming from the forward (dashed line) and backward (dot-dashed line) RPA amplitudes for the 0_1^+ (top panel) and 0_2^+ (bottom panel) states.

least, spectroscopic factors of the two-nucleon transfer (p,t) and (t,p) reactions. To compute all these quantities we adopted the QPM which enabled us also to explore the RPA constituent phonons of the 0^+ states and the quasiparticle structure of the low-lying 0^+ RPA phonons.

We found that an appreciable fraction of the QPM 0^+ states have large, if not dominant, two-phonon components, mostly built out of collective octupole phonons, in agreement with previous IBM predictions. The small $E2$ and $E0$ strengths obtained confirm the lack of quadrupole collectivity predicted by the PSM for all the 0^+ states. Most of the low-lying 0^+ states are linear combinations of several, huge in some cases, two-quasiparticle $q\overline{q}$ components. Not all these states, however, display pairing collectivity. The quasiparticle components, in fact, act coherently only in the first excited 0_1^+. As a result, only this state is predicted to be strongly populated in (p,t) two-nucleon transfer reactions. The same 0_1^+ state is predicted to be strongly populated also in (t,p) reactions. The latter result strongly suggests that the 0^+ states of ^{158}Gd are not pairing isomeric states.

For a more reliable conclusion, we need to solve the discrepancy concerning the energy distribution of the transfer transition strengths. As already pointed out, the large QPM strength is concentrated in the first 0_1^+, while the large experimental one is collected by the second excited 0_2^+. Also the available experimental $E0$ and $E2$ spectra suggest an energy inversion among these two states. Achieving this goal might be a hard task. We may enlarge the phonon space and hope that the coupling with some phonon configurations, excluded in the space considered here, invert the energies of the two 0^+ states. Another possible route is dictated by the complexity of the RPA 0^+ states. It is not excluded, in fact, that the $K^\pi=0^+$ phonons contain non-negligible hexadecapole or even higher $\lambda\mu$ multipole components, not accounted for in the RPA $K^\pi=0^+$ states computed here. The coupling between the $\lambda\mu=20$ and, say, $\lambda\mu=40$ phonons might promote the energy inversion between the two lowest $K^\pi=0^+$ phonons. If such an upgrading is not sufficient, it remains to reexamine the criteria for fixing the Hamiltonian parameters. The experimental data, used as a guide for the fit, leave some freedom for varying the multipole pairing strength constants. Also, it might be necessary to generate the single particle spectrum directly for the odd neighbors of ^{158}Gd rather than using the $A=155$ nuclei as done here. This latter strategy is suggested by the high sensitivity of the spectroscopic factors to the Hamiltonian parameters. Their sharp dependence on deformation, shown in the paper, is an example. Investigations along these routes are under way.

It might be also useful to extend the QPM investigations to other nuclei on the wake of the new exciting results provided by more recent (p,t) experiments [2,3]. A systematic and detailed comparative analysis might provide the guidelines for improving the theoretical description of these 0^+ states and, thereby, gaining a better understanding of their complex structure.

ACKNOWLEDGMENTS

This work was partly supported by the Italian Ministero dell'Istruzione, Universitá and Ricerca (MIUR) and RFBR Grant No. 03-02-17395. It is a pleasure to thank A. Aprahamian, R. F. Casten, and G. Graw for useful discussion and, once more, G. Graw for having sent us the spectroscopic factors extracted from the cross sections published in Ref. [1].

[1] S. R. Lesher, A. Aprahamian, L. Trache, A. Oros-Peusquens, S. Deyliz, A. Gollwitzer, R. Hertenberger, B. D. Valnion, and G. Graw, Phys. Rev. C **66**, 051305(R) (2002).
[2] H.-F. Wirth, G. Graw, S. Christen, D. Cutoiu, Y. Eisermann, C. Günther, R. Hertenberger, J. Jolie, A. I. Levon, O. Möller, G. Thiamova, P. Thirolf, D. Tonev, and N. V. Zamfir, Phys. Rev. C **69**, 044310 (2004).
[3] G. Graw (private communication).
[4] N. V. Zamfir, Jing-ye Zhang, and R. F. Casten, Phys. Rev. C **66**, 057303 (2002).
[5] Y. Sun, A. Aprahamian, J. Zhang, and C. Lee, Phys. Rev. C **68**, 061301(R) (2003).
[6] V. G. Soloviev, *Theory of Atomic Nuclei: Quasiparticles and Phonons* (Institute of Physics, Bristol, 1992).
[7] D. R. Bes and R. A. Broglia, Nucl. Phys. **80**, 289 (1966).
[8] R. A. Broglia, D. R. Bes, and B. S. Nilsson, Phys. Lett. **50B**, 213 (1972).
[9] I. Ragnarsson and R. A. Broglia, Nucl. Phys. **A263**, 315

(1976).
[10] R. F. Casten, E. R. Flynn, J. D. Garrett, O. Hansen, T. J. Mulligan, D. R. Bess, R. A. Broglia, and B. Nilsson, Phys. Lett. **40B**, 333 (1972).
[11] V. G. Soloviev, Z. Phys. A **334**, 143 (1989).
[12] V. G. Soloviev, A. V. Sushkov, and N. Yu. Shirikova, Nucl. Phys. **A568**, 244 (1994).
[13] F. A. Gareev, S. P. Ivanova, V. G. Soloviev, and S. I. Fedotov, Sov. J. Part. Nucl. **4**, 357 (1973).
[14] V. G. Soloviev, A. V. Sushkov, and N. Yu. Shirikova, Z. Phys. A **358**, 287 (1997).
[15] V. G. Soloviev, A. V. Sushkov, and N. Yu. Shirikova, Phys. Rev. C **56**, 2528 (1997).
[16] W. Nazarewicz, M. A. Riley, and J. D. Garrett, Nucl. Phys. **A512**, 61 (1990).
[17] R. G. Helmer, Nucl. Data Sheets **101**, 325 (2004).
[18] J. L. Wood, E. F. Zganjar, C. De Coester, and K. Heyde, Nucl. Phys. **A651**,323 (1999).
[19] P. E. Garrett, J. Phys. G **27**, R1 (2001).
[20] R. C. Greenwood, C. W. Reich, H. A. Baader, H. R. Koch, D. Breitig, O. W. B. Schult, B. Fogelberg, A. Bäcklin, W. Mampe, T. Von Egidy, and K. Schreckenbach, Nucl. Phys. **A304**, 327 (1978).
[21] G. Løvhøiden, T. F. Thorsteinsen, E. Andersen, M. F. Kiziltan, and D. G. Burke, Nucl. Phys. **A494**, 157 (1989).